Quantifying the Structural Changes of Perfluorosulfonated Acid Ionomer upon Reaction with Hydroxyl Radicals

Lida Ghassemzadeh and Steven Holdcroft[**]

Department of Chemistry, Simon Fraser University, 8888 University Drive, Burnaby, British Columbia, Canada V5A1S6

Ⓢ *Supporting Information*

ABSTRACT: We report molecular-level quantification of chemical degradation of perfluorosulfonated acid (PFSA) ionomer membranes. This is made possible by determining the structure of Nafion 211 using calibrated ^{19}F magic angle spinning nuclear magnetic resonance spectroscopy upon exposure to hydroxyl radicals. Individual segments of the ionomer were monitored to show that the backbone is resistant to hydroxyl radical attack and that degradation occurs solely on the side chain, with the most significant attack occurring toward the end of the side chain. The method provides a means to evaluate changes in chemical structure of PFSA ionomers with a much higher degree of certainty than previously possible.

The lifetime of polymer electrolyte membrane fuel cells (PEMFC) depends largely on the stability of the polymer electrolyte membrane and is a critical issue in the commercialization of PEMFC technology.[1−3] Perfluorosulfonated acid (PFSA) ionomer membranes, such as Nafion, are the most widely used electrolyte material for PEMFCs. The ionomer comprises a PTFE backbone to provide mechanical stability and fluorous−ether side chains bearing a sulfonic acid to provide proton conductivity.[4] Recent in situ and ex situ ESR spectroscopic studies confirm the formation of free radicals and their reactivity during the fuel cell operation as the main reason for chemical degradation of the membrane.[5−10] Inside the fuel cell, hydroxyl radical originates from electrochemical and chemical reactions at both the anode and the cathode. OH radicals form by decomposition of hydrogen peroxide (produced from a two-electron oxygen reduction) via transition metal cations or thermally.[11,12] They are also formed by reaction of H_2 and O_2 on the surface of Pt catalyst as a result of gas crossover through the membrane.[13−17] It is suggested that earlier versions of Nafion PFSA ionomer membrane chemically degrade through OH radical attack on carboxylic acid groups present at the terminus of the main chain,[13,18−20] or through OH radical attack at the C−S or O−C bonds in the side chain.[13,19−27] "Chemically stabilized" grades of Nafion, e.g., Nafion 211, were developed for which the concentration of terminal carboxylic acid groups was decreased to negligible levels.[18,19]

Typical indicators for chemical degradation of PFSA ionomers include a decrease in ion exchange capacity, proton conductivity, or membrane thickness. The quantitative method of choice used for detecting chemical degradation is fluoride release measurements in outlet water streams from fuel cells, reported as a fluoride emission rate (FER). However, FER is a poor representative for the structural change in PFSA ionomers because fluorine is present in different parts of the structure. Fluoride release from the main chain leads to relatively small decreases in ion exchange capacity (IEC) and conductivity, whereas fluoride release from the side chain leads to dramatic decreases. Moreover, FER quantifies only one product of degradation, F^-, and organofluorine compounds, e.g., fluorinated side chains, are not detected.

In this work we use solid-state ^{19}F NMR spectroscopy in a quantified manner to study chemical degradation of a representative PFSA ionomer, Nafion 211, in the presence of hydroxyl radicals generated using Fenton's reagent. A calibration curve for quantifying solid-state ^{19}F NMR spectra was constructed using sodium hexafluorosilicate (Na_2SiF_6) (^{19}F-rich) and SiO_2 (^{19}F-free) as reference compounds. Both compounds were dried at 110 °C for 12 h and ground to a fine powder before mixing to a specific mass ratio. Mixed reference powders were packed in a Bruker 2.5 mm zirconia rotor with Vespel drive tips and caps. Solid-state ^{19}F NMR experiments were performed at 376.09 MHz on a Bruker 400 MHz spectrometer operating at a static magnetic field of 9.4 T. A 2.5 mm three-channel HFX wide-band magic angle spinning (MAS) probe with a Vespel spinning module was used. Spectra were recorded at 300 K at a spinning rate of 30 kHz, with a 90° pulse length of 3.0 μs, a recycle delay of 3 s, and a dwell time of 5 μs. A total of 256 transients were recorded, each acquired for 4096.24 ms with a spectral width of 227 kHz (∼600 ppm). The spectra were processed with TOPSPIN software, and the free induction decay (FID) was Fourier transformed without any additional line broadening. The chemical shifts were calibrated with respect to trichlorofluoromethane ($CFCl_3$), having a resonance at 0.0 ppm.

The signal-to-noise ratio (S/N) of the recorded spectra was >27 000. [19]F spectra of reference samples with different wt% Na_2SiF_6 are shown in the Supporting Information. The spectra are divided by the sample mass to an accuracy of 1 μg.

The chemical environments of all fluorine atoms in the octahedral structure of SiF_6^{2-} are identical; thus a single peak at −151.45 ppm is observed. The integrated area of the peak (and side bands) is directly proportional to molar concentration of fluorine.[28,29] A linear fit between the calculated integral of the peak and the fluorine concentration is observed ($R^2 = 0.9986$). This plot is used to quantify chemical changes in PFSA ionomer (see Supporting Information). Multiple Nafion 211

membranes were immersed into individual solutions of Fenton's reagent (20 vol% H_2O_2, 10 ppm Fe^{2+}, renewed every 12 h) at 80 °C, to provide a source of hydroxyl radicals. Membranes were extracted at different times and thoroughly washed in 1 M H_2SO_4 at 80 °C and deionized water. The membranes were dried at 110 °C for 12 h under vacuum, and NMR analyses were performed under identical conditions as described for the Na_2SiF_6/SiO_2 mixtures.

Figure 1 presents the spectra of pristine Nafion 211. Peak assignment is based on a previous analysis.[30] The spectrum was
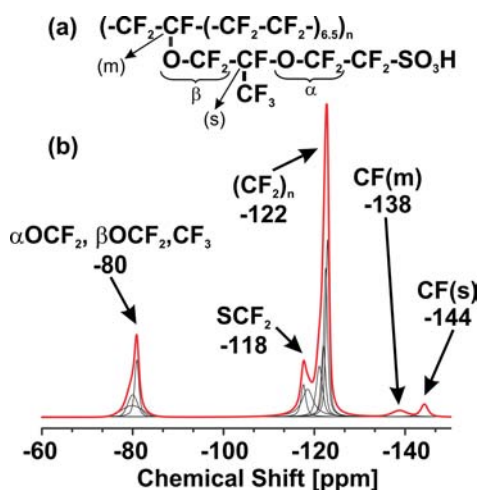
Figure 1. (a) Chemical structure of pristine Nafion 211. (b) ^{19}F MAS NMR spectrum (red line) and peak assignment of Nafion 211. The deconvoluted spectrum is shown in black.

deconvoluted using the *dmfit* program.[31] Peak positions, line shapes, and error margins are shown in Table 1. The most intense signal occurs at −122 ppm, which is an overlap of different signals due to main-chain CF_2 units. The differences in chemical shift values and line broadenings result from their varied distances from the side-chain branch point.[30] The broader peaks are related to CF_2 groups closer to the branch point (see the figure in Supporting Information).

Other signals are as follows: signals for the two different OCF_2 groups and the CF_3 group overlap at −80 ppm; a signal at −118 ppm due to SCF_2; and peaks at −138 and −144 ppm due to main-chain and side-chain CF groups, CF(m) and CF(s), respectively.

The signal at −80 ppm was deconvoluted into three peaks with relative areas of 2:2:3. The two signals with similar area are due to OCF_2 groups, and the peak with the larger area is due to CF_3. The narrower peak is assigned to the OCF_2 near the end of the side chain (α-OCF_2), and the broader signal is due to the OCF_2 near the branch point (β-OCF_2). This assignment is based on the expected mobility of these groups and is in agreement with former [19]F−^{13}C 2D NMR analyses of Nafion.[30]

The sum of all the integrals (including the side bands) is a function of total fluorine content. The intensity of the spectra was divided by the mass of each sample, and the fluorine content of each fluorine-containing unit was determined using the calibration plot. Unlike previous ^{19}F MAS NMR studies of Nafion in which spectra are normalized to the integral of the main-chain signal at −122 ppm,[13,24,25] normalization to mass presented in this work has the distinct advantage of providing absolute quantification of changes in the side chain and main chain. The fluorine concentration associated with each fluorine-containing unit as a function of exposure time to free radicals is shown in Figure 2a. The concentration of main-chain CF_2 (the sum of five peaks with the estimation error of ±1.5%) was unchanged upon exposure to Fenton's reagent for 48 h. In contrast, the side chain clearly degrades. The largest change in fluorine content was observed for the side-chain SCF_2 groups, which decreased steadily with exposure to free radicals. Over a period of 48 h, 14% of the SCF_2 groups were cleaved from the ionomer (see Figure 2b). Comparing the side-chain CF (−144 ppm) and main-chain CF (−138 ppm) concentrations before and after exposure to radicals indicates the main-chain CF peak is unchanged, whereas the side-chain CF group concentration decreases by 11%. Comparing the concentration of OCF_2 groups, it was found that α-OCF_2 decrease at a similar rate as the SCF_2 group (15% loss over 48h), while the β-OCF_2 decreases more slowly (8% after 48 h). The changes in concentration of the SCF_2 and α-OCF_2 appear earlier into the Fenton's reagent experiment (e.g., after 12 h), while the changes to the β-OCF_2 and the side-chain CF and CF_3 units appear at advanced stages of reaction (after 24 h), implying free radical attack is more prevalent close to the ionic head groups. This is consistent with results of a comparative study between Nafion (long side-chain ionomer) and Hyflon Ion (short side chain) membranes, where the absence of the −O−CF_2−$CF(CF_3)$− fragment in the side chain of the latter improved side-chain stability.[24,25] Danilczuk et al.[32] showed that while chemically stabilized Nafion ionomer (comprising reduced terminal carboxylic acid content) is slightly less reactive to OH radical attack compared to unstabilized Nafion, 3M short side-chain ionomer membranes are less reactive to OH radicals by a factor of 20. A kinetic study on perfluorinated model compounds also concludes that the main point of attack by OH radical is likely to be α-OCF_2.[27]

The precision of this method is further demonstrated by calculating the IEC from the SCF_2 concentration and comparing the values to those determined by conventional titration. IEC values of all samples, pristine and chemically degraded, are comparable, as shown in Figure 3. The decrease of IEC as a function of exposure time indicates that the loss in IEC is a direct consequence of the loss of SCF_2 groups.

In regard to the mechanism of chemical degradation, two possible scenarios are considered. The first mechanism,

Table 1. Deconvoluted ^{19}F NMR Signals for Pristine Nafion 211[a]

	β-OCF_2	α-OCF_2	CF_3	SCF_2	CF_2 (n)					CF(m)	CF(s)
position (ppm)	−79.9	−80.0	−80.9	−117.6	−118.5	−121.1	−122.0	−122.5	−122.9	−138.8	−144.2
relative area	2	2	3	2	4	4	4	8	8	1	1
width (kHz)	2.01 ± 0.2	0.95 ± 0.1	0.41 ± 0.03	0.46 ± 0.04	1.13 ± 0.2	0.61 ± 0.1	0.43 ± 0.08	0.38 ± 0.06	0.32 ± 0.06	1.47 ± 0.05	0.7 ± 0.02
G/L	1	1	0.3	0.8	0	0.4	0.4	0.4	0.4	0.3	0.6

[a]G/L is Gaussian:Lorentzian ratio in peak shape. For assignments see Figure 1. (m) and (s) represent main chain and side chain, respectively.
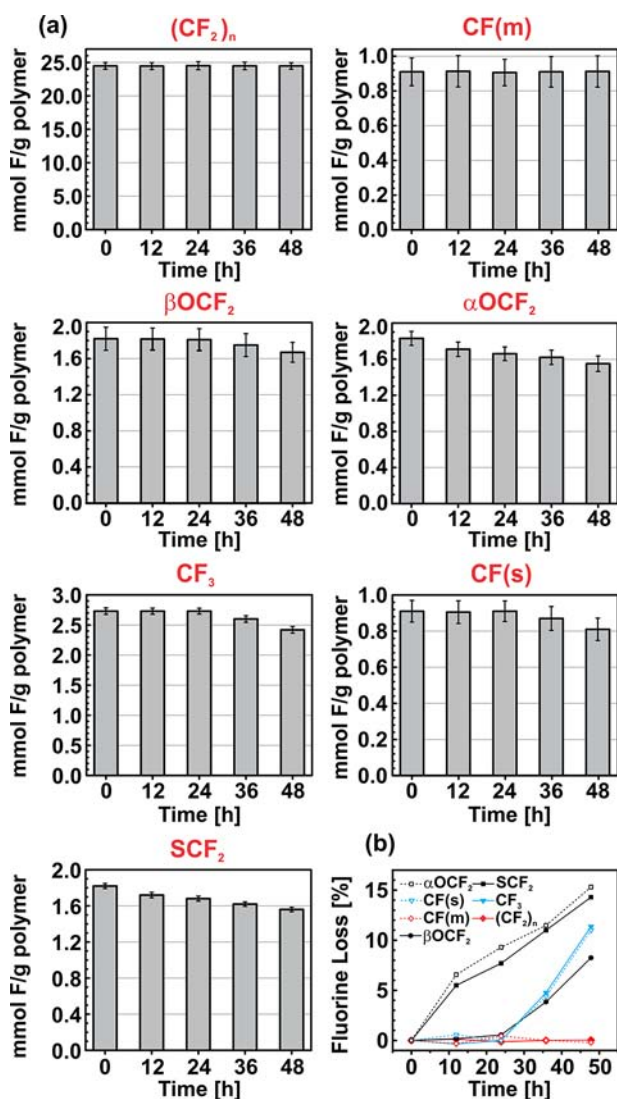
Figure 2. (a) Fluorine concentration and (b) fluorine loss associated with each fluorine-containing unit in Nafion 211 as a function of exposure time to Fenton's reagent. The error margins of the data in (b) are similar to those in (a). (See also Table S1 of Supporting Information.)
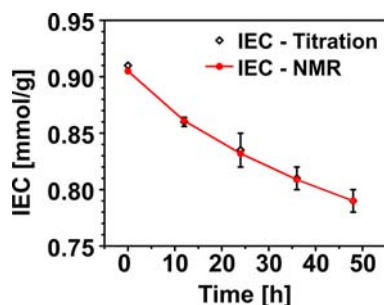
Figure 3. Comparison the IEC values of Nafion 211 membranes calculated from NMR-derived SCF_2 concentrations and by titration.

proposed by Yu et al.[26] using density functional theory (DFT) calculations, is based on attack of OH radicals on the C−S bond and formation of $R\text{-}OCF_2CF_2^{\bullet}$, which is unstable and leads to O−C bond cleavage (Figure 4a). The cleavage of C−S as the weakest bond in the polymer has been formerly discussed as an initial point of attack leading to side-chain
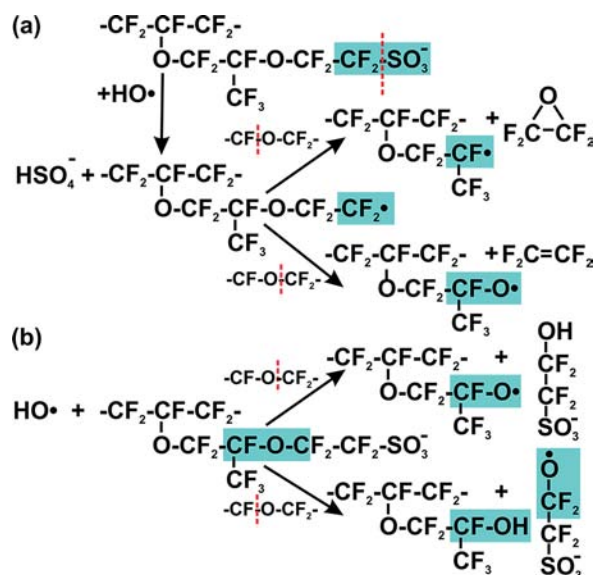
Figure 4. Proposed mechanisms for the side-chain degradation of Nafion 211 by OH radical: (a) attack of the C−S bond and indirect cleavage of the O−C bond in $\alpha\text{-}OCF_2$ or (b) direct attack of the α-OCF_2.

degradation.[13,20,33] Subsequent transformation leading to a loss of an epoxide or tetrafluoroethylene can explain the similar rate of loss observed for the α-OCF_2 and the SCF_2 units only if the α-O−C bond cleavage is fast enough.

A recent DFT calculation suggests that, despite the cleavage of the C−S bond being the most exothermic, hydroxyl radical attack at this point may be kinetically hindered.[33] In another DFT study, comparing the reaction of OH radicals with fluorinated model compounds showed that the cleavage of the ether bond is more favorable than cleavage of the C−S bond.[34] These results are consistent with experimental work by Danilczuk et al. on the formation of $^{\bullet}OCF_2R$ radicals in spin trap analyses of fluorinated model compound $CF_3CF_2OCF_2CF_2SO_3$.[35] It is also consistent with the kinetic study by Dreizler et al. on model compounds, in which they concluded the main point of attack by OH radical is α-OCF_2. A mass spectroscopic analysis showed no evidence for the reaction of sulfonic acid groups with OH radicals.[19]

Based on these reports and our quantified analysis, the more likely mechanism is that represented in Figure 4b, involving direct attack of a OH radical on the α-C−O bond, although it is unknown whether the C−O or O−C bond is cleaved. This mechanism explains the similar rate of fluorine loss in the α-OCF_2 unit and the SCF_2 group. Although this is the first point of attack, further degradation involves the CF(s) and β-OCF_2 units, as observed in NMR data of samples treated longer than 24 h. More details of this are provided in Figure S3 in the Supporting Information.

In summary, quantitative ^{19}F MAS NMR data show that the main chain of Nafion 211 is indeed stable against the OH radical attack and that the α-OCF_2 group is likely the first point of attack by oxygenated radicals. Moreover, the technique is proven reliable and accurate and can be used for comparing the durability of all forms of PFSA ionomers, including shorter side-chain ionomers such as Aquivion and 3M membranes.

ASSOCIATED CONTENT

Ⓢ Supporting Information

NMR calibration plot, peak line width, advance stages of chemical degradation, original NMR spectra of the samples before and after exposure to Fenton's reagent, and fluorine loss as a function of time. This material is available free of charge via the Internet at http://pubs.acs.org.

AUTHOR INFORMATION

Corresponding Author

holdcrof@sfu.ca

Notes

The authors declare no competing financial interest.

ACKNOWLEDGMENTS

REFERENCES

(1) Rodgers, M. P.; Bonville, L. J.; Kunz, H. R.; Slattery, D. K.; Fenton, J. M. *Chem. Rev.* **2012**, *112*, 6075−6103.

(2) Buechi, F. N.; Inaba, M.; Schmidt, T. J. *Polymer Electrolyte Fuel Cell Durability*; Springer: Berlin, 2009.

(3) Wu, J. F.; Yuan, X. Z.; Martin, J. J.; Wang, H. J.; Zhang, J. J.; Shen, J.; Wu, S. H.; Merida, W. *J. Power Sources* **2008**, *184*, 104−119.

(4) Mauritz, K. A.; Moore, R. B. *Chem. Rev.* **2004**, *104*, 4535−4585.

(5) Danilczuk, M.; Coms, F. D.; Schlick, S. *J. Phys. Chem. B* **2009**, *113*, 8031−8042.

(6) Panchenko, A.; Dilger, H.; Kerres, J.; Hein, M.; Ullrich, A.; Kaz, T.; Roduner, E. *Phys. Chem. Chem. Phys.* **2004**, *6*, 2891−2894.

(7) Bosnjakovic, A.; Schlick, S. *J. Phys. Chem. B* **2004**, *108*, 4332−4337.

(8) Kadirov, M. K.; Bosnjakovic, A.; Schlick, S. *J. Phys. Chem. B* **2005**, *109*, 7664−7670.

(9) Bosnjakovic, A.; Kadirov, M. K.; Schlick, S. *Res. Chem. Intermed.* **2007**, *33*, 677−687.

(10) Danilczuk, M.; Bosnjakovic, A.; Kadirov, M. K.; Schlick, S. *J. Power Sources* **2007**, *172*, 78−82.

(11) Pozio, A.; Silva, R. F.; De Francesco, M.; Giorgi, L. *Electrochim. Acta* **2003**, *48*, 1543−1549.

(12) Okada, T.; Satou, H.; Yuasa, M. *Langmuir* **2003**, *19*, 2325−2332.

(13) Ghassemzadeh, L.; Kreuer, K.-D.; Maier, J.; Müller, K. *J. Phys. Chem. C* **2010**, *114*, 14635.

(14) Mittal, V. O.; Kunz, H. R.; Fenton, J. M. *J. Electrochem. Soc.* **2007**, *154*, B652−B656.

(15) Mittal, V. O.; Kunz, H. R.; Fenton, J. M. *J. Electrochem. Soc.* **2006**, *153*, A1755−a1759.

(16) Xie, J.; Wood, D. L.; More, K. L.; Atanassov, P.; Borup, R. L. *J. Electrochem. Soc.* **2005**, *152*, A1011−A1020.

(17) Endoh, E. *Electrochem. Solid State Lett.* **2004**, *7*, A209−A211.

(18) Curtin, D. E.; Lousenberg, R. D.; Henry, T. J.; Tangeman, P. C.; Tisack, M. E. *J. Power Sources* **2004**, *131*, 41−48.

(19) Zhou, C.; Guerra, M. A.; Qiu, Z. M.; Zawodzinski, T. A.; Schiraldi, D. A. *Macromolecules* **2007**, *40*, 8695−8707.

(20) Coms, F. D. *ECS Trans.* **2008**, *16*, 235−255.

(21) Delaney, W. E.; Liu, W. *ECS Trans.* **2007**, *11*, 1093−1104.

(22) Takasaki, M.; Nakagawa, Y.; Sakiyama, Y.; Tanabe, K.; Ookubo, K.; Sato, N.; Minamide, T.; Nakayama, H.; Hori, M. *ECS Trans.* **2009**, *17*, 439−447.

(23) Tokumasu, T.; Ogawa, I.; Koyama, M.; Ishimoto, T.; Miyamoto, A. *ECS Trans.* **2009**, *25*, 765−772.

(24) Ghassemzadeh, L.; Marrony, M.; Barrera, R.; Kreuer, K. D.; Maier, J.; Müller, K. *J. Power Sources* **2009**, *186*, 334−338.

(25) Ghassemzadeh, L.; Kreuer, K. D.; Maier, J.; Müller, K. *J. Power Sources* **2011**, *196*, 2490−2497.

(26) Yu, T. H.; Sha, Y.; Liu, W.-G.; Merinov, B. V.; Shirvanian, P.; Goddard, W. A. *J. Am. Chem. Soc.* **2011**, *133*, 19857−19863.

(27) Dreizler, A. M.; Roduner, E. *Fuel Cells* **2012**, *12*, 132−140.

(28) Pauli, G. F.; Jaki, B. U.; Lankin, D. C. *J. Nat. Prod.* **2004**, *68*, 133−149.

(29) Fry, R. A.; Tsomaia, N.; Pantano, C. G.; Mueller, K. T. *J. Am. Chem. Soc.* **2003**, *125*, 2378−2379.

(30) Chen, Q.; Schmidt-Rohr, K. *Macromolecules* **2004**, *37*, 5995−6003.

(31) Massiot, D.; Fayon, F.; Capron, M.; King, I.; Le Calvé, S.; Alonso, B.; Durand, J.-O.; Bujoli, B.; Gan, Z.; Hoatson, G. *Magn. Reson. Chem.* **2002**, *40*, 70−76.

(32) Danilczuk, M.; Perkowski, A. J.; Schlick, S. *Macromolecules* **2010**, *43*, 3352−3358.

(33) Kumar, M.; Paddison, S. J. *J. Mater. Res.* **2012**, *27*, 1982−1991.

(34) Ishimoto, T.; Nagumo, R.; Ogura, T.; Ishihara, T.; Kim, B.; Miyamoto, A.; Koyama, M. *J. Electrochem. Soc.* **2010**, *157*, B1305−B1309.

(35) Danilczuk, M.; Coms, F. D.; Schlick, S. *Fuel Cells* **2008**, *8*, 436−452.